SYMMETRIES OF MONOCORONAL TILINGS

DIRK FRETTLÖH AND ALEXEY GARBER

Abstract. The vertex corona of a vertex of some tiling is the vertex together with the adjacent tiles. A tiling where all vertex coronae are congruent is called monocoronal. We provide a classification of monocoronal tilings in the Euclidean plane and derive a list of all possible symmetry groups of monocoronal tilings. In particular, any monocoronal tiling with respect to direct congruence is crystallographic, whereas any monocoronal tiling with respect to congruence (reflections allowed) is either crystallographic or it has a one-dimensional translation group. Furthermore, bounds on the number of the dimensions of the translation group of monocoronal tilings in higher dimensional Euclidean space are obtained.

arXiv:1402.4658v1 [math.MG] 19 Feb 2014

1. Introduction

The question how local properties determine global order of spatial structures arises naturally in many different contexts. If the structures under consideration are crystallographic structures, for instance, tilings are used frequently as models for these structures. In this context, one studies how local properties of a tiling determine its global properties.

To mention just a few results in this context for tilings: A tiling is called *monohedral* if all tiles are congruent. A tiling is called *isohedral* if its symmetry group acts transitively on the tiles. Hilbert's 18th problem asked whether there is a tile admitting a monohedral tiling, but no isohedral tiling. (In fact, Hilbert asked the question for tilings in three dimensions.) Heesch gave an affirmative answer in 1935 by proposing a planar non-convex tile with this property [12], [11]. A classification of all isohedral tilings by convex polygons was obtained by Reinhardt [13], see also Section 9 of the wonderful book by Grünbaum and Shephard [11]. In contrast, a classification of all monohedral tilings by convex polygons has not been obtained yet. For instance, it is still unknown which types of convex pentagons admit monohedral tilings of the Euclidean plane [11, Section 9].

In a similar manner, a *monogonal* tiling is one in which each vertex star — i.e., a vertex together with its incident edges — is congruent to any other vertex star. A tiling is called *isogonal*, if its symmetry group acts transitively on the vertex stars. A classification of isogonal tilings is contained in [11, Section 6]. There are 11 combinatorial types of isogonal tilings and 91 types of (unmarked, normal) isogonal tilings altogether. Each of the 11 combinatorial types of isogonal tilings can be realised by an *Archimedean* (aka *uniform*) tiling, that is a vertex transitive tiling by regular polygons (which then is automatically isogonal) [11, Section 2].

The Local Theorem for tilings yields a necessary and sufficient criterion for a tiling to be crystallographic in terms of the number and the symmetries of k-th tile coronae in the tiling [7]. (The 0th tile corona of a tile T is T itself. The k-th tile corona of T is the set of all tiles sharing a facet with some tile of the $k-1$-th tile corona of T.) As a consequence of this result, a monohedral tiling is isohedral if and only if all first tile coronae in $\mathcal{T}$ are congruent [8].

In light of the facts above it seems natural to explore tilings in which all vertex coronae are congruent. We will call these tilings *monocoronal*. The *vertex corona* of a vertex x in a tiling is x together with the tiles incident to x. Thus, monocoronal is a stronger property than monogonal.

The main results of this paper are obtained for tilings in the Euclidean plane $\mathbb{R}^2$ (Section 2). It turns out that a tiling in $\mathbb{R}^2$ is necessarily isogonal (hence crystallographic) if all vertex corona are directly congruent (i.e., mirror images forbidden). This is stated in Theorem 2.1. In contrast, if all vertex corona of some tiling $\mathcal{T}$ are congruent, but not necessarily directly congruent (i.e., mirror images allowed), then the translation subgroup of the symmetry group of $\mathcal{T}$ can be one-dimensional. In particular, $\mathcal{T}$ may be neither crystallographic nor isogonal. This is Theorem 2.2. These results

are obtained using a complete classification of monocoronal tilings. This classification is contained in Appendices A and B.

In Section 3 the results of Section 2 are used to obtain some monocoronal tilings in higher dimensional Euclidean space with small translation groups. Section 4 briefly illustrates the situation in hyperbolic spaces and states some suggestions for further work.

1.1. Definitions and Notations. Let $\mathbb{X}$ be a Euclidean space $\mathbb{R}^d$ or a hyperbolic space $\mathbb{H}^d$. A *tiling* is a countable collection $\{T_1, T_2, \ldots\}$ of compact sets T_i (the *tiles*) that is a covering (i.e., $\bigcup_i T_i = \mathbb{X}$) as well as a packing (i.e. $\mathring{T}_i \cap \mathring{T}_j = \varnothing$ if $i \neq j$, where $\mathring{T}$ denotes the interior of T). Here the tiles will almost always be convex polytopes; if not, it is mentioned explicitly. A *vertex* of a tiling $\mathcal{T}$ is a point x such that x is a vertex of at least one tile in $\mathcal{T}$. Note that in general (higher dimensions, non-convex tiles) a proper definition of a vertex of a tiling can be problematic, compare [11] or [10]. Our definition is tailored to monocoronal tilings. It agrees with the usual definitions and properties of a vertex of a tiling if one considers only planar tilings by convex polygons. For instance, x is a vertex of a tiling $\mathcal{T}$ if and only if x is an isolated point of the intersection of some tiles in $\mathcal{T}$; or: every vertex of a tile (in the usual sense: vertex of a polygon) is a vertex of the tiling, compare [10].

A tiling is called *face-to-face* if the intersection of two tiles is always an entire face (possibly of dimension less than d, possibly empty) of both of the tiles. In particular, planar tilings by convex polygons are face-to-face if the intersection of two tiles is either an entire edge of both of the tiles, or a vertex of both of the tiles, or empty.

Definition 1.1. *Let x be a vertex in some tiling $\mathcal{T}$. The* vertex-corona *of x is the set of all tiles $T \in \mathcal{T}$ such that $x \in T$, together with x.*

In tilings by non-convex tiles, two different vertices may have the same set of adjacent tiles. Thus it is necessary to keep track of the defining vertex x in the definition of the vertex corona.

Definition 1.2. *If all vertex-coronae in a tiling $\mathcal{T}$ are directly congruent (mirror images forbidden), then we say that $\mathcal{T}$ is a* monocoronal tiling up to rigid motions. *If all vertex-coronae in a tiling $\mathcal{T}$ are congruent (mirror images allowed), then we say that $\mathcal{T}$ is a* monocoronal tiling up to congruence. *If it is clear from the context which of the both terms is meant then we will say briefly that $\mathcal{T}$ is a* monocoronal tiling.

The *symmetry group* of a tiling $\mathcal{T}$ is the set of all isometries $\varphi : \mathbb{X} \to \mathbb{X}$ such that $\varphi(\mathcal{T}) = \mathcal{T}$. In the sequel we are interested in possible symmetry groups of monocoronal tilings. In particular we ask whether only crystallographic groups can occur.

Definition 1.3. *A tiling in $\mathbb{R}^d$ is called k-*periodic *if the symmetry group contains exactly k linearly independent translations. A 0-periodic tiling is called* non-periodic.

Definition 1.4. *The tiling $\mathcal{T}$ is called* crystallographic *if its symmetry group has compact fundamental domain. Otherwise it is called* non-crystallographic.

In Euclidean space $\mathbb{R}^d$ the two notions "crystallographic" and "d-periodic" are equivalent.

Theorem 1.5 (Bieberbach, 1911-1912, [2, 3])**.** *A tiling $\mathcal{T}$ of $\mathbb{R}^d$ is crystallographic iff it is d-periodic.*

Since in hyperbolic spaces there is no natural meaning of "translation" it does not make sense to speak of "periodic" or "non-periodic" tilings in $\mathbb{H}^d$. Nevertheless we can ask whether a hyperbolic monocoronal tiling is necessarily crystallographic. This is answered in Section 4.

We will use orbifold notation to denote planar symmetry groups in the sequel, compare [5]. For instance, $*442$ denotes the symmetry group of the canonical face-to-face tiling of $\mathbb{R}^2$ by unit squares. For a translation of orbifold notation into other notations see [5] or [14]. In orbifold notation the 17 crystallographic groups in the Euclidean plane ("wallpaper groups") are

$$*632,\ *442,\ *333,\ *2222,\ **,\ *\times,\ \times\times,\quad 632,\ 442,\ 333,\ 2222,\ \circ,\quad 4*2,\ 3*3,\ 2*22,\ 22*, 22\times;$$

and the seven frieze groups are

$$\infty\infty,\ *\infty\infty,\ \infty*,\ \infty\times,\ 22\infty,\ 2*\infty,\ *22\infty.$$

2. Euclidean plane

This section is dedicated to the question: What are possible symmetry groups of monocoronal tilings in $\mathbb{R}^2$? It turns out that the answer is rather different depending on whether we consider monocoronal tiling up to rigid motions, or up to congruence. In the sequel the main results are stated first. It follows a subsection containing an outline of the classification of all monocoronal tilings that are face to face, then a subsection sketching the classification of monocoronal tilings that that are not face-to-face, and finally the proofs of Theorems 2.1 and 2.2 are given.

Theorem 2.1. *Every monocoronal tiling up to rigid motions has one of the following 12 symmetry groups:*

$$*632,\ *442,\ *333,\ *2222,\quad 632,\ 442,\ 333,\ 2222,\quad 4*2,\ 3*3,\ 2*22,\ 22*.$$

In particular, every such tiling is crystallographic, every such tiling has a center of rotational symmetry of order at least 2, and its symmetry group acts transitively on the vertices.

Theorem 2.2. *Every monocoronal tiling up to congruence is either 1-periodic, or its symmetry is one out of 16 wallpaper groups: any except $*\times$. If such tiling is 1-periodic then its symmetry group is one of four frieze groups: $\infty\infty$, $\infty\times$, $\infty*$, or 22∞. In particular, every such tiling is crystallographic or 1-periodic.*

Remark 2.3. It turns out that the 1-periodic tilings in Theorem 2.2 consist of 1-periodic layers that are stacked according to a non-periodic one-dimensional sequence (see for instance Figure 9, page 11). Such a sequence may look simply like $\dots 1,1,1,0,1,1,1,\dots$ (all 1s, one 0) or, more interestingly, like a non-periodic Fibonacci sequence $\dots 0,1,1,0,1,0,1,1,0,1,1,0,1,0\dots$, where each finite subsequence occurs infinitely often with bounded gaps. The study of nonperiodic symbolic sequences is an interesting field of study on its own, compare for instance [9] or [1].

2.1. Face-to-face tilings. We start with determining the possible combinatorial types of vertex coronae in a monocoronal tiling; that is, in which way can every vertex be surrounded by n-gons. This first part is already contained in [11]: Our Lemma 2.4 corresponds to Equation (3.5.5) in [11], our Table 1 corresponds to Table 2.1.1 in [11] (which is also applicable to the more general case considered here). For the sake of completeness we include the line of reasoning in the sequel.

Lemma 2.4. *Let $\mathcal{T}$ be a monocoronal tiling such that every vertex is incident to n polygons with $a_1,\dots,a_n$ many edges, respectively. Then*

$$\sum_{i=1}^{n}\frac{1}{a_i}=\frac{n}{2}-1.$$

Proof. Let k_i denote the number of i-gons in the corona of a vertex in a monocoronal tiling $\mathcal{T}$. Consider the average sum of angles at every vertex. On one hand, it is equal to 2π since $\mathcal{T}$ is a tiling. On the other hand, every i-gon adds an angle $\frac{i-2}{i}\pi$ in average. By summing up contributions of all polygons and dividing by π we obtain $\sum_{i\geq 3}\frac{k_i(i-2)}{i}=2$. Let n denote the total number of polygons incident to a vertex x in $\mathcal{T}$ (i.e. $n=\sum k_i$) then this identity becomes

$$\sum_{i\geq 3}\frac{k_i}{i}=\frac{n}{2}-1.$$

Reformulating this with respect to a_i yields the claim. □

One can easily check that the equation in Lemma 2.4 is possible only in the cases listed in Table 1 (where only non-zero k_i's are listed).

Not all cases with $n=3$ and $n=4$ can be realized by a tiling in the Euclidean plane. Impossible cases are marked by (i) in Table 1. For example, there is no tiling in the Euclidean plane such that every vertex is incident to one triangle, one 7-gon and one 42-gon. Indeed, the edges of any triangle in such a tiling in cyclic order would belong alternately to 7-gons and to 42-gons. Since a triangle has an odd number of edges this is impossible.

$n = 6$	$k_3 = 6$	
$n = 5$	$k_3 = 4$, $k_6 = 1$	
	$k_3 = 3$, $k_4 = 2$	
$n = 4$	$k_3 = 2$, $k_4 = 1$, $k_{12} = 1$	(i)
	$k_3 = 2$, $k_6 = 2$	
	$k_3 = 1$, $k_4 = 2$, $k_6 = 1$	
	$k_4 = 4$	
$n = 3$	$k_3 = 1$, $k_7 = 1$, $k_{42} = 1$	(i)
	$k_3 = 1$, $k_8 = 1$, $k_{24} = 1$	(i)
	$k_3 = 1$, $k_9 = 1$, $k_{18} = 1$	(i)
	$k_3 = 1$, $k_{10} = 1$, $k_{15} = 1$	(i)
	$k_3 = 1$, $k_{12} = 2$	(i)
	$k_4 = 1$, $k_5 = 1$, $k_{20} = 1$	(i)
	$k_4 = 1$, $k_6 = 1$, $k_{12} = 1$	
	$k_4 = 1$, $k_8 = 2$	
	$k_5 = 2$, $k_{10} = 1$	(i)
	$k_6 = 3$	

TABLE 1. Possible combinatorial types of vertex coronae following from Lemma 2.4. Cases that are impossible for further reasons are marked with (i).

In the same way one can prove that if $n = 3$ then only four cases can be realized: one triangle and two 12-gons, or three hexagons, or one quadrilateral and two octagons, or one quadrilateral, hexagon and one 12-gon. If $n = 4$ then the case with two triangles, one quadrilateral and one 12-gon cannot be realized.

The full list of all possible monocoronal face-to-face tilings presented in Appendix A. In the sequel the general line of reasoning is illustrated by a detailed discussion of a typical example, namely the case where the vertex corona consists of one triangle, two quadrilaterals, and one hexagon.

First we consider the topological structure of a tiling $\mathcal{T}$ with prescribed (combinatorial) polygons in the corona of every vertex. For example, if $n = 6$ then the tiling $\mathcal{T}$ will be combinatorially equivalent to the tiling with regular triangles.

The example under consideration — one triangle, two quadrilaterals, one hexagon — is less trivial. In this case with there are two possible combinatorial coronas. They are shown in Figure 1. The

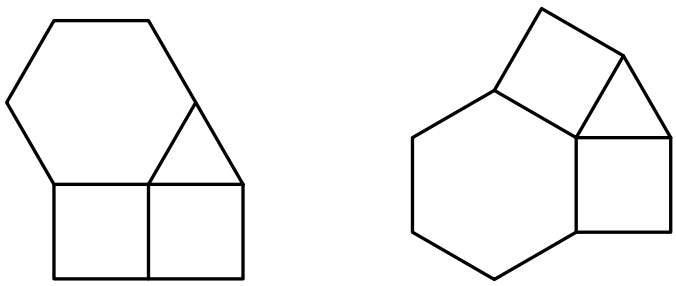

FIGURE 1. Two theoretical cases of local structure with triangle, two quadrilaterals and hexagon.

constellation in the left part of the figure can not be realized in any tiling of the plane. The reason is the same as above: quadrilaterals and hexagons need to alternate in a cyclic way along the edges of some triangle, yielding a contradiction. So the topological structure of the tiling that we are looking for will be the same as in Figure 2.

The next step is to mark equal edges or predefined angles. (This is the point where we go beyond [11].) For example, in the unique topologically possible corona with triangle, two quadrilaterals and hexagon there is only one angle of triangle in every vertex, therefore all angles of all triangles in our tiling are equal to $\frac{\pi}{3}$. By the same reason all angles of all hexagons are equal to $\frac{2\pi}{3}$.

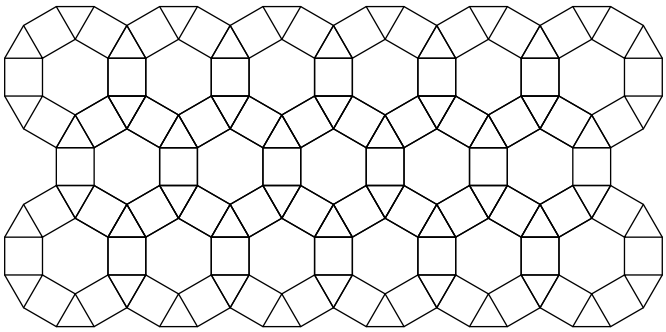

FIGURE 2. Topological structure of a tiling with unique vertex corona consisting of a triangle, two quadrilaterals and a hexagon.

We use the same strategy to mark edges of equal length. It is easy to see that all edges of all triangles are equal, since every corona contains only one equilateral triangle. Hence we mark all edges of all triangles with red color. The two edges of a hexagon that are incident to a given vertex x may be of different lengths. Thus we mark them with blue and green, respectively. Then the edges of all hexagons are colored alternating with blue and green since every vertex must be incident to one blue and one green edge of a hexagon. Hence we have colored all edges in the corona except two of them (see Figure 3).

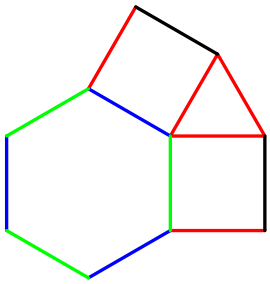

FIGURE 3. Intermediate coloring of corona.

Both uncolored edges belong to some hexagons so they can be blue or green. First we will consider the case when green and blue are equal. Then both quadrilaterals in every corona are parallelograms. There are no more than two different angles in total in these quadrilaterals since in one corona there are only two angles of quadrilaterals. So metrically the corona of an arbitrary vertex x looks as follows (see Figure 4): a regular hexagon, two equal parallelograms that touch x with different angles (or equal iff they are rectangles), and a regular triangle.

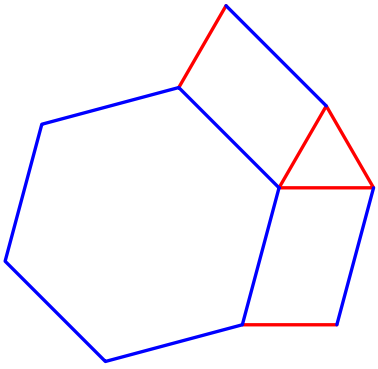

FIGURE 4. First possible case of a corona with one triangle, two quadrilaterals, and one hexagon.

If the blue and the green edges are of different length then one of the uncolored edges in Figure 3 is green and the other one is blue. There are two arguments for that. The first one which works in this

particular case is the following: if both edges are of the same color, say blue, then every corona does not have a green edge on the outer part of incident quadrilaterals, which is impossible. The second argument is general for all monocoronal tilings: in any corona with center x, the portion of green edges of quadrilaterals containing x is the same as the portion of green edges of quadrilaterals not containing x. This means in this example: one quarter of all edges of quadrilaterals must be green.

So there are two possibilities of coloring all edges of the vertex corona under consideration. These are shown in Figure 5.

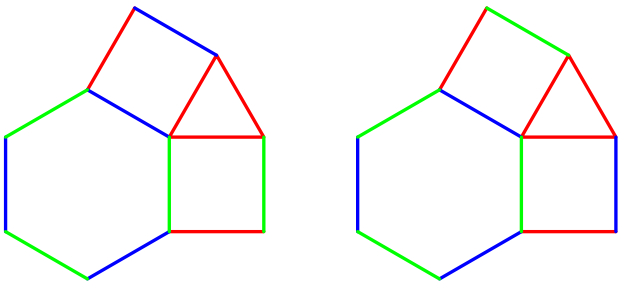

FIGURE 5. Possible colorings of corona.

In the left image both quadrilaterals are parallelograms. Moreover, every corona contains only one angle between red and blue edges, hence all these angles are equal. But four such angles are angles of one quadrilateral, so this quadrilateral is a rectangle. By the same reason the second quadrilateral is a rectangle, too. Now if we consider an arbitrary triangle then it is surrounded by rectangles that alternate cyclically along its edges: a rectangle with two red and two green edges is followed by a rectangle with two red and two blue edges. Again, since the triangle has an odd number of edges, this yields a contradiction.

By the same reason, in the right image all angles between red and blue edges are equal, and all angles between red and green edges are equal. So both quadrilaterals are equal isosceles trapezoids. Hence the metrical picture looks like shown in Figure 6.

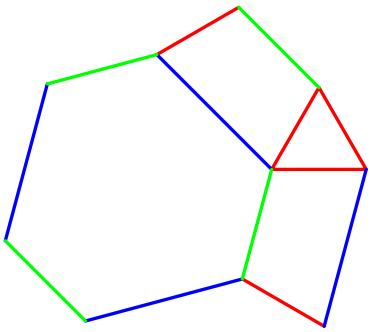

FIGURE 6. The second possible corona with triangle, two quadrilaterals, and hexagon.

Putting everything together we obtain that there are two families of different monocoronal tilings whose vertex corona consists of one triangle, two quadrilaterals, and one hexagon. Both families are shown in Figure 7. Both families admit only crystallographic tilings since the metrical structure is uniquely defined by the structure of an arbitrary corona satisfying Figures 4 or 6.

Proceeding in this manner for all possible cases yields the list of tilings in Appendix A.

2.2. Non face-to-face tilings. In the case of non-face-to-face tilings we can prove a lemma similar to Lemma 2.5. We assume that each vertex x is contained in the relative interior of the edge of some polygon P_x. It is clear that there is exactly one such polygon.

Lemma 2.5. *If there is a monocoronal tiling $\mathcal{T}$ such that every vertex is a vertex of polygons with number of edges $\{a_1, \dots, a_n\}$ and lies in a side of one more polygon then*

$$\sum \frac{1}{a_i} = \frac{n-1}{2}.$$

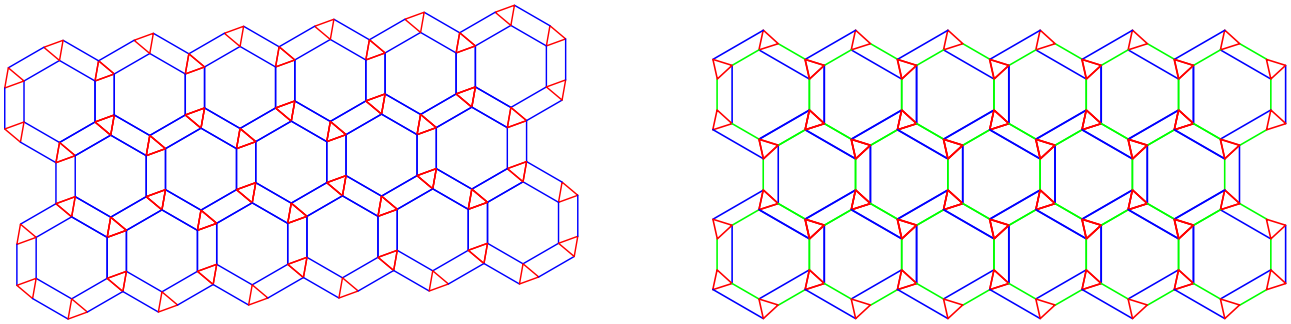

FIGURE 7. Families of monocoronal tilings with one triangle, two quadrilaterals, and one hexagon.

Proof. Let k_i denote the number of i-gons (not including P_x) in the corona of the vertex x in a monocoronal tiling $\mathcal{T}$. Consider the average sum of angles at every vertex, excluding the contribution of P_x. On one hand, it is equal to π since $\mathcal{T}$ is a tiling and P_x contributes an angle equal to π. On the other hand, every i-gon adds an angle $\frac{i-2}{i}\pi$ in average. After summing up contributions of all polygons and dividing by π we obtain

$$\sum_{i\geq 3} \frac{k_i(i-2)}{i} = 1.$$

Reformulating this with respect to a_i yields the claim. □

One can easily check that the equation in Lemma 2.5 is possible only in the following cases (we will list only non-zero k_i's):

$$n = 3 :\ k_3 = 3, \qquad n = 2 :\ k_3 = 1, k_6 = 1, \quad \text{or} \quad n - 2 :\ k_4 = 2.$$

Now we can use the same technique as in 2.1 for obtaining the full list of all possible monocoronal non face-to-face tilings, see Appendix B.

2.3. Proofs of the main theorems. The full list of tilings in Appendices A and B allows us to complete the proofs of Theorems 2.1 and 2.2.

Proof (of Theorem 2.1). The first assertion can be checked by going through the list in Appendix A, omitting those tilings that require reflected coronae (i.e., consider only those figures with (D) in the caption). We cannot find each group directly depicted in the figures. But many figures cover an entire class of special cases. For instance, Figure 15 — showing a triangle tiling with five different edge lengths — covers also the special cases of four, three, two and one different edge lengths. In particular, the tiling in Figure 15 with all edge lengths equal shows the regular triangle tiling by equilateral triangles with symmetry group $*632$. In this flavor, the following table shows the number of a figure in which the corresponding symmetry group occurs, together with some additional constraint if necessary. To see that this table is complete, one has to verify that the groups $22\times$, $**$, $*\times$, $\times\times$ and $\circ$ are not symmetry groups of the tilings in the list (again only considering figures with (D) in the caption). The simplest way is to check that all these tilings do have a centre of 2-fold or 3-fold rotation. This rules out $**$, $*\times$, $\times\times$ and $\circ$. Then one may check which figures show glide reflections, but no reflections: this is true for none of the figures considered here. This rules out $22\times$ and shows all assertions except the last claim.

It remains to check the figures (again only the ones with (D) in the caption) for vertex transitivity. This is done easily since all tilings considered are crystallographic: only the vertices in a fundamental domain of the translation group have to be checked for equivalence with respect to the symmetry group. In most cases an appropriate rotation will suffice. To give an example, consider Figure 18: The translations in the symmetry group of the depicted tiling act transitively on the small triangles. A 3-fold rotation about the centre of a small triangle permutes the vertices of this small triangle cyclically. Any vertex in the tiling is the vertex of some small triangle. Thus a composition of some

$*632$	15, all edge lengths equal
$*442$	28, all edge lengths equal
$*333$	25, all interior angles of the hexagons equal
$*2222$	28, all rectangles congruent
632	24
442	22
333	18
2222	15
$4 * 2$	23, with squares and half-squares
$3 * 3$	18, all triangles isosceles (red=blue)
$2 * 22$	19, with squares and equilateral triangles
$22 *$	15, with red=violet, green=yellow.

TABLE 2. Symmetry groups with the number of their corresponding figures and further specifications.

translation and some rotation — which is again a rotation — maps any given vertex to any different vertex. □

Proof (of Theorem 2.2). The assertion can be checked by going through the full list in Appendix A. In the figures one finds 13 crystallographic groups as symmetry groups of the depicted tilings (the 12 groups from the last proof together with $22\times$). The following short list gives for each group G occurring the number of one or two figures in the appendix such that G is the symmetry group of the corresponding tiling. Note that all symmetry groups can be realized with face-to-face tilings.

$*632$	$*442$	$*333$	$*2222$	632	442	333	2222	$4 * 2$	$3 * 3$	$2 * 22$	$22 *$	$22\times$
39	41	45	28	24, 26	22, 36	18, 25	15, 16	33, 43	27, 38	29, 52	30, 46	16, 32

TABLE 3. Symmetry groups with the number of their corresponding figures

The remaining three crystallographic groups $**$, $\times\times$ and $\circ$ are realised by families of tilings that allow also non-crystallographic tilings. This is true for the tilings depicted in Figures 17, 20, 21, 34, 55, and 60.

In the four cases where the tilings are face-to-face, non-crystallographic symmetry groups can occur since the tilings consist of alternating layers such that each second layer is mirror symmetric. The symmetric layers consist either of isosceles triangles (I) or of rectangles (R), as depicted in Figure 8. The other layers come in two chiral versions and consist either of parallelograms (P_0 and P_1) or

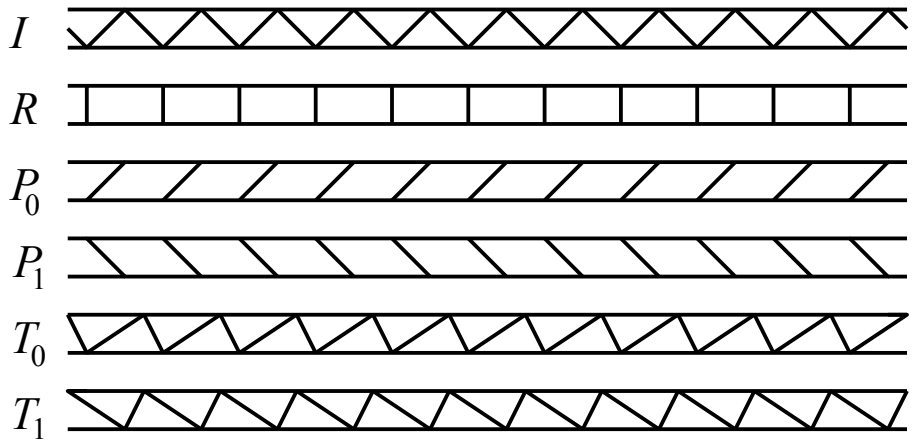

FIGURE 8. Layers of isosceles triangles (I), layers of rectangles (R), layers of parallelograms (P_i) and layers of non-isosceles triangles (T_i).

of triangles (T_0 and T_1), see Figure 8. The tilings corresponding to Figure 17 consist of alternating

layers of the form

$$\dots I, T_{i_{-1}}, I, T_{i_0}, I, T_{i_1}, I, T_{i_2}, \dots, \quad (i_k \in \{0,1\}),$$

the tilings corresponding to Figure 20 consist of alternating layers of the form

$$\dots I, P_{i_{-1}}, I, P_{i_0}, I, P_{i_1}, I, P_{i_2}, \dots, \quad (i_k \in \{0,1\}),$$

the tilings corresponding to Figure 21 consist of alternating layers of the form

$$\dots R, T_{i_{-1}}, R, T_{i_0}, I, P_{i_1}, I, P_{i_2}, \dots, \quad (i_k \in \{0,1\}),$$

and the tilings corresponding to Figure 34 consist of alternating layers of the form

$$\dots R, P_{i_{-1}}, R, P_{i_0}, R, P_{i_1}, R, P_{i_2}, \dots, \quad (i_k \in \{0,1\}).$$

In all cases the sequence $i := (i_k)_{k\in\mathbb{Z}}$ can be chosen arbitrarily in $\{0,1\}^{\mathbb{Z}}$. The symmetry group of the corresponding tilings depend on the sequence i. In particular, if i is a non-periodic symbolic sequence, the symmetry group of the corresponding tiling has translations only parallel to the layers. (The symbolic sequence $i = (i_k)_{k\in\mathbb{Z}}$ is called *non-periodic*, if $i_k = i_{k+m}$ for all $k \in \mathbb{Z}$ implies $m = 0$.)

By choosing a periodic sequence i appropriately tilings with symmetry groups $**$, $\times\times$ and $\circ$ can be realised. To construct concrete examples we use tilings by parallelograms and rectangles. These tilings are depicted in Appendix C. For instance, $i = \dots 101100\ 101100\ 101100 \dots$ yields tilings with symmetry group $**$ (no rotations, two reflections in mirror axes parallel to the layers, see Figure 64). Choosing $i = \dots 111011000100\ 111011000100\ 111011000100 \dots$ yields tilings with symmetry group $\times\times$ (no rotations, glide reflections with mirror axes orthogonal to the layers, no reflections, see Figure 65). With $i = \dots 0001011\ 0001011\ 0001011 \dots$ we obtain tilings with symmetry group $\circ$ (translations only, see Figure 66).

In order to see that these examples do actually have the claimed symmetry groups, it is instructive to consider how certain isometries act on the symbolic sequence i. Here i denotes the sequence of the original tiling, then i' is the sequence of the tiling after applying the isometry.

- Reflection in a line orthogonal to the layers switches the symbols 1 and 2: $i'_k \equiv i_k + 1 \mod 2$.
- Reflection in a line parallel to the layers switches the symbols 1 and 2 and reverses the order: $i'_k \equiv i_{-k} + 1 \mod 2$.
- Rotation by π (around the mid-point of a short edge of some tile in layer 0) reverses the order: $i'_k = i_{-k}$.
- Translation orthogonal to the layers by $2m$ layers shifts by m: $i'_k = i_{k+m}$.

In particular, if the sequence i is not invariant under any operation mentioned above then the corresponding tiling is not invariant under the corresponding isometry. Keeping this in mind it is easy to check that the tilings in Figures 64, 65 and 66 have the claimed symmetry groups.

It remains to rule out tilings with symmetry groups $*\times$ in the cases considered here, i.e., in the six families of tilings that may have non-crystallographic symmetry groups. Since these tilings consist of the layers discussed above, any possible reflection mapping the tiling to itself has to map the layers to themselves. Thus its mirror axis is either parallel to the layers, or orthogonal to the layers. A reflection orthogonal to the layers maps a layer P_1 to a layer P_2, resp. a layer T_1 to a layer T_2, thus it cannot be a symmetry of the tiling. Hence any possible reflection must have a mirror axis parallel to the layers.

Since the reflection maps entire layers to entire layers, the mirror axis lies either on the boundary of some layer, or in the central axis of some layer. In the first case, the reflection would switch a symmetric layer (I or R) with a non-symmetric layer (P_i or T_i), hence it is not a symmetry of the tiling. In the second case, it cannot be the central axis of a layer P_i, or T_i, or I, since these are not mirror symmetric with respect to reflection about their central axis. Thus the mirror axis of a possible reflection is the central axis of a layer R.

From the list of the 17 wallpaper groups we obtain that the mirror axis of a possible glide reflection is parallel to the axis of the mirror reflection in the symmetry group $\times*$. Hence the axis of any glide reflection is parallel to the layers. By the same reasoning as above, it must be the central axis of a layer R consisting of rectangles. It remains to show that there is no "original" such glide reflection, in terms of group generators. I.e., we have to show that any such glide reflection is a combination of a reflection r and a translation t that are already symmetries of the tiling.

The translational part of any glide reflection as above maps rectangles to rectangles. Thus its length is an integer multiple of the length of one edge of the rectangles in layer R. But a translation by just one edge length of the rectangles already maps the tiling to itself. Thus for any possible glide reflection g which translational part shifts by k rectangles, there is a translation t — shifting by $-k$ rectangles — such that $t \circ g$ is a proper reflection that maps the tiling to itself.

Hence a group $*\times$ cannot occur as symmetry group of a monocoronal tiling.

Now we will establish all possible symmetry groups of 1-periodic monocoronal tilings. First we will give examples as sequences of layers of rectangles and parallelograms as before (sequences of 0's and 1's). For the group $\infty\infty$ we can use the sequence $\ldots 0001101000 \ldots$ with only three 1's. For the group $\infty *$ we can use the sequence $\ldots 00001111 \ldots$ which is infinity with 0's in one direction and 1's in the other. And for the group 22∞ we can use the sequence $\ldots 000010000 \ldots$ with only one 1.

The group $\infty\times$ can occur as a symmetry group of tiling with layers of isosceles triangles and parallelograms with sequence $\ldots 00001111 \ldots$ which is infinity with 0's in one direction and 1's in the other. Here the axis of the glide reflection is in the middle line of layers of triangles between 0 and 1.

All other three frieze groups $*\infty\infty$, $2 * \infty$, and $*22\infty$ can not be realized as symmetry group of 1-periodic monocoronal tiling because they contain a mirror symmetry in the direction orthogonal to layers which is impossible for both types of non-symmetric layers. □

3. Euclidean space of dimension 3 and higher

In the last section we have seen that monocoronal tilings up to rigid motions are always 2-periodic, whereas monocoronal tilings in general are either 1-periodic or 2-periodic. Thus one may ask for the possible dimensions of the translation group of a monocoronal tiling in higher dimension $d \geq 3$. Trivially, the maximal dimension is always d, realised for instance by the canonical face-to-face tiling of $\mathbb{R}^d$ by unit hypercubes. Thus this section gives upper bounds for the minimal possible dimension of translation groups of monocoronal tilings in $\mathbb{R}^d$ for $d \geq 3$, distinguishing the cases of face-to-face (Theorem 3.1) vs non face-to-face (Theorem 3.2). Both case split further with respect to direct congruence vs congruence. In analogy to the plane case, two sets $A, B \subset \mathbb{R}^d$ are called *congruent*, if there is $t \in \mathbb{R}^d$ such that $A = t + RB$ for some $R \in O(d)$. A and B are called *directly congruent*, if there is $t \in \mathbb{R}^d$ such that $A = t + RB$ for some $R \in SO(d)$. The latter corresponds to the existence of a rigid motion of $\mathbb{R}^d$ moving A to B.

Theorem 3.1. *There are face-to-face tilings of $\mathbb{R}^d$ that are $\lceil \frac{d}{2} \rceil$-periodic and monocoronal.*
There are face-to-face tilings of $\mathbb{R}^d$ that are $\lceil \frac{d+1}{2} \rceil$-periodic and monocoronal up to rigid motions.

Proof. For the first claim, consider a 1-periodic monocoronal tiling $\mathcal{T}$ of the Euclidean plane (e.g. Figure 9. Consider the direct product $\mathcal{T} \times \ldots \times \mathcal{T}$ of $\lfloor \frac{d}{2} \rfloor$ copies of $\mathcal{T}$. This yields a $\lfloor \frac{d}{2} \rfloor$-periodic monocoronal tiling. If d is odd then we need to take one additional direct product with some 1-periodic tiling of $\mathbb{R}^1$ (for example a tiling of the line by unit intervals).

For the second claim, note that the Cartesian product $A \times B$ is directly congruent if either A or B is directly congruent. Let $\mathcal{T}$ be the direct product of a 1-periodic tiling from Figure 34 with a tiling of $\mathbb{R}^1$ by unit intervals. Then $\mathcal{T}$ is a monocoronal tiling up to rigid motions of $\mathbb{R}^3$. The product of $\mathcal{T}$ with k copies of any 1-periodic monocoronal tiling of $\mathbb{R}^2$ is a monocoronal tiling up to rigid motions of $\mathbb{R}^{3+2k}$ that is $2 + k$-periodic. If d is odd, then $d = 3 + 2k$ for some k, and $\mathcal{T}$ is $\lceil \frac{d+1}{2} \rceil$-periodic. If d is even then consider the additional direct product with a further tiling of $\mathbb{R}^1$ by unit intervals. This yields a $\lceil \frac{d+1}{2} \rceil$-periodic monocoronal tiling up to rigid motions of $\mathbb{R}^d$ for all $d \geq 3$. □

For the non face-to-face case one can even push it further: one can construct non-periodic tilings in $\mathbb{R}^d$ for $d \geq 3$.

Theorem 3.2. *For any $d \geq 3$ there are non-periodic non face-to-face tilings of $\mathbb{R}^d$ that are monocoronal.*
For any $d \geq 4$ there are non-periodic non face-to-face tilings of $\mathbb{R}^d$ that are monocoronal up to rigid motions .

Proof. We will start with the first claim. We will show the construction of such an example in $\mathbb{R}^3$. It can easily be generalised to higher dimensions.

We start with a 1-periodic tiling from Figure 21 where all rectangles are unit squares and all triangles are isosceles right triangles with edges $1, 1, \sqrt{2}$ (see Figure 9). Using this tiling we can create a *layer* L

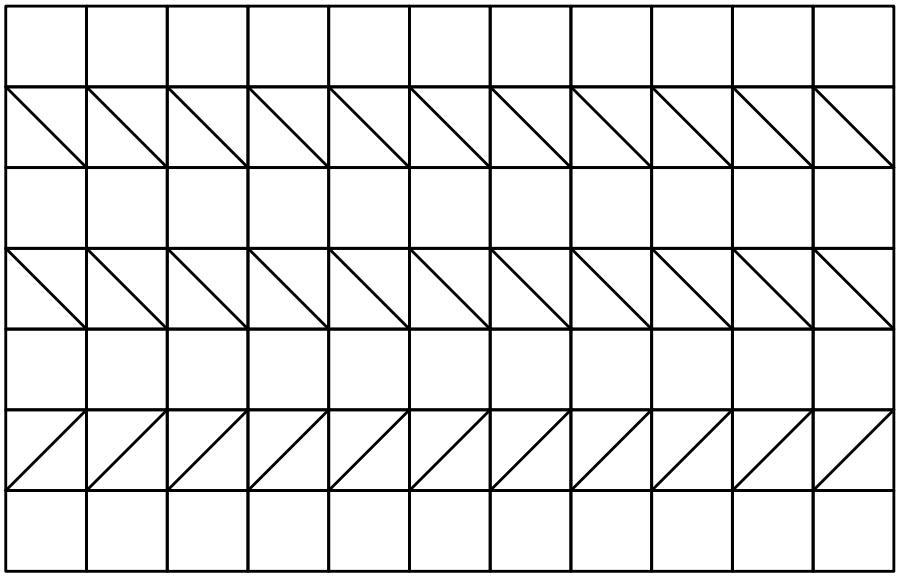

FIGURE 9. Building block for an non-periodic tiling.

by taking its direct product with an orthogonal unit interval (see Figure 10). This layer is 1-periodic. In the next step we add a layer of unit cubes below the layer L (see Figure 11). This is the point

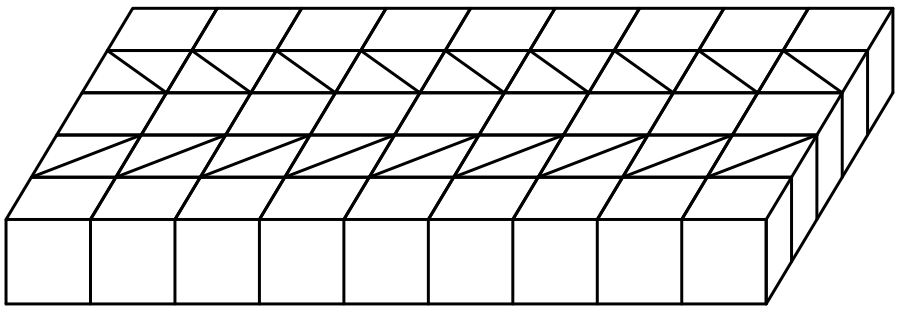

FIGURE 10. Layer of unit cubes and triangular prisms.

where our tiling starts to be non face-to-face. In the next step (see Figure 12) we add one more layer

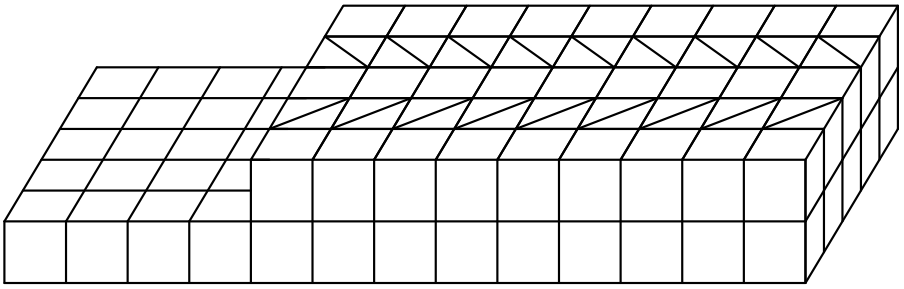

FIGURE 11. Layer L and layer of unit cubes.

congruent to L below that is rotated by $\frac{\pi}{2}$ with respect to L. This latter layer is 1-periodic, but in a

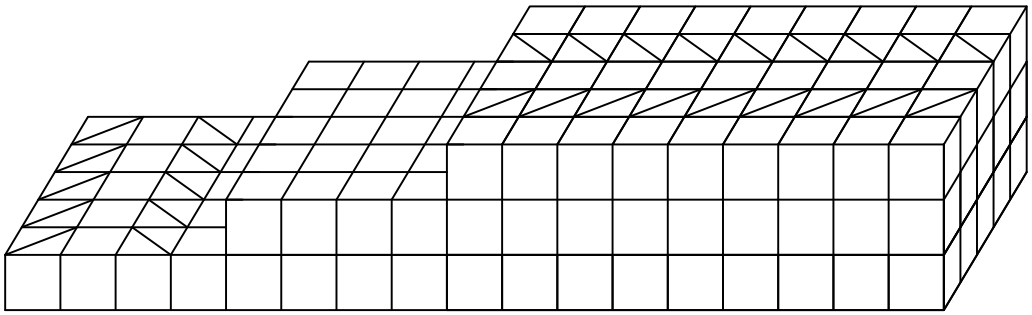

FIGURE 12. Three layers of unit cubes, two of them contains cubes cut into prisms.

direction orthogonal to the period of the first layer. Hence the union of all three layers is non-periodic. Proceeding in this manner yields a tiling of $\mathbb{R}^3$ such that even layers consist of unit cubes, odd layers consist of unit cubes and triangular prisms. It is clear that any vertex corona consists of four unit cubes from some even layer, two unit cubes from an adjacent odd layer, and three prisms. Hence the tiling is a monocoronal tiling.

In each step of the construction one may choose a layer that is a translate of L, or a copy of L rotated by $\frac{\pi}{2}$. If the sequence of choices is non-periodic then the tiling has no period in the vertical direction. Hence we obtain a non-periodic tiling.

The constructed tiling is not a monocoronal tiling up to rigid motions, so for the second claim of the theorem we need to modify the construction a little bit. As for the first claim, we will present a construction for $\mathbb{R}^4$ that can be easily generalised to higher dimensions.

Again, we start from the tiling by unit squares and right isosceles triangles in Figure 9. In a preliminary step we take the direct product of this tiling with a tiling of the orthogonal line by unit intervals. This yields a 2-periodic tiling of $\mathbb{R}^3$ where each vertex corona consists of unit cubes and triangular prisms, and each vertex corona is mirror-symmetric.

Taking the direct product of this tiling with an orthogonal unit interval yields a layer L' in $\mathbb{R}^4$ consisting of unit 4-cubes and prisms over triangular prisms. Now we can repeat the steps from the proof of the first claim of Theorem 3.1. Every even layer of the tiling consists of unit 4-cubes, and every odd layer is a directly congruent copy of the layer L', preserving the "almost" cubical structure on its boundary.

The initial 3-dimensional tiling was monocoronal, with mirror-symmetric corona. Thus the resulting tiling is also monocoronal with mirror-symmetric corona, hence it is a monocoronal tiling up to rigid motion. We can force this tiling to be non-periodic by taking some non-periodic sequence of rotations of L' for odd layers. L' is 2-periodic so in every step we can choose one direction in which the copy of L' is non-periodic. It suffices to choose each of three directions at least once to destroy any period parallel to the layers. □

4. Conclusion

This short conclusion mentions some open problems in the context of this paper that are still open and may suggest further work.

The smallest possible dimension of the translation group of monocoronal face-to-face tilings of Euclidean spaces of dimension at least 3 is still unknown: it is 0, 1 or 2. In particular, the question "Does there exist a non-periodic monocoronal face-to-face tiling in $\mathbb{R}^3$" is still open.

Throughout this paper we restrict our study only to convex tiles, but the same question could be asked for tilings with non-convex polygons (resp. polytopes) as well. Allowing non-convex polygons does not change the classification of two-dimensional face-to-face monocoronal tiling in Appendix A: every possible monocoronal tiling using non-convex polygons is already covered by the classification. For non face-to-face tiling it is even easier, because in this case no angle of any polygon can be greater than π, hence no monocoronal non-face-to-face tiling with non-convex polygons is possible at all.

One may also ask for classifications of monocoronal tilings in other spaces of constant curvature, in particular in hyperbolic space. For instance we might ask: Is it true that every monocoronal tiling of $\mathbb{H}^d$ is crystallographic? It is easier to answer this question for hyperbolic spaces than for Euclidean spaces since there is a family of non-crystallographic tilings of $\mathbb{H}^d$ with unique tile corona. This tiling can be used to construct tilings with unique vertex corona, that is, monocoronal tilings.

Theorem 4.1. *There is a non-crystallographic face-to-face tiling of $\mathbb{H}^d$ that is monocoronal up to congruence.*

Proof. Here we show the construction for $\mathbb{H}^2$. An analogous construction works for arbitrary dimension.

We start from (one of) Böröczky tiling $\mathcal{B}$ [4]. It is a non-crystallographic tiling of hyperbolic plane [6, Theorem. 4.4] by equal pentagons. Figure 13 shows a schematic view of this tiling as a tiling of the representation of $\mathbb{H}^2$ as lower half plane.

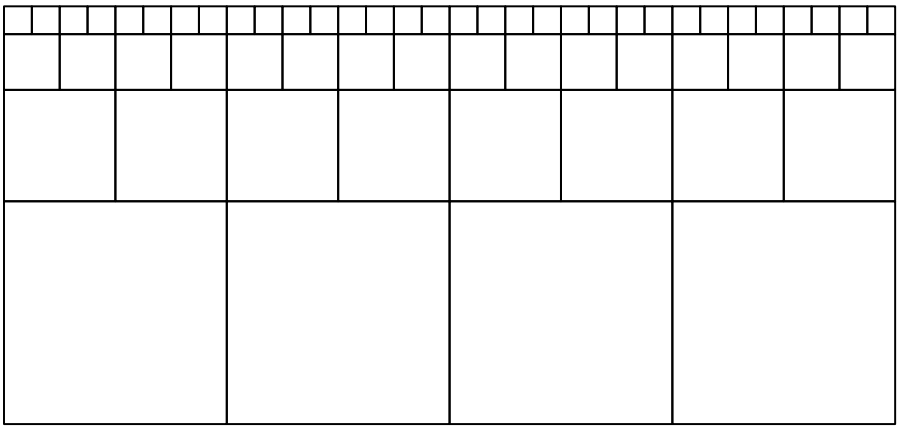

FIGURE 13. Example of Böröczky tiling.

It is easy to see that this tiling $\mathcal{B}$ is not monocoronal. But every tile is surrounded by other tiles "in the same way", so we can use it to construct a monocoronal tiling. We construct the *dual tiling* by taking barycenters of the initial tiles as vertices of a new tiling and new tiles are convex hulls of vertices corresponding to "old" tiles incident to one "old" vertex.

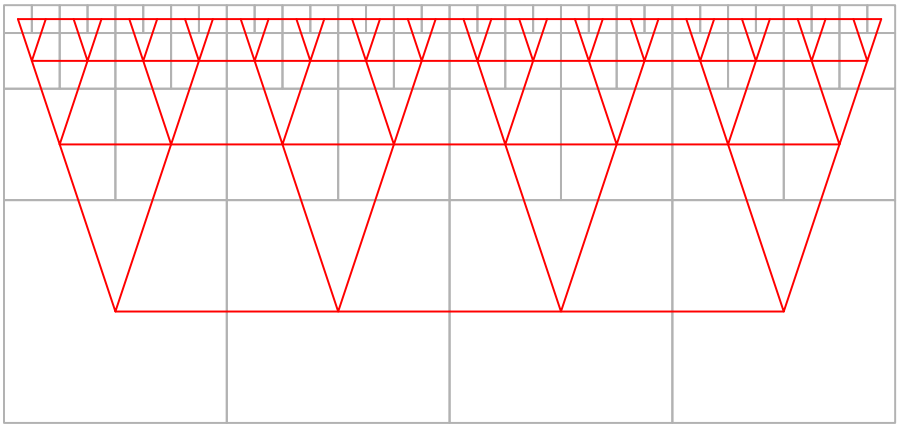

FIGURE 14. Dual to Böröczky tiling.

For arbitrary tilings this construction does not necessary yield a (face-to-face) tiling, but in the case of Böröczky tiling it works. Barycenters of tiles of one "horizontal layer" lie on one horocycle (horosphere in $\mathbb{H}^d$). Thus tiles of the dual tiling form a layer structure between neighboring horocycles. Moreover, this tiling is a monocoronal tiling, since in the original tiling all first tile-coronae are congruent. The dual tiling is non-crystallographic, since the initial Böröczky tiling was non-crystallographic. □

Theorem 4.1 shows that face-to-face tilings in $\mathbb{H}^d$ that are monocoronal up to congruence can be non-crystallographic (in a pretty strict sense: their symmetry group being finite, see [6]). They can also be crystallographic for small d, any regular tiling of $\mathbb{H}^d$ yields an example.

The same question with respect to monocoronal tilings up to rigid motions is still open: The vertex coronae of the tilings in Figure 14 are congruent, but not directly congruent. It might also be interesting to study the situation in the higher dimensional analogues of the Böröczky tilings.

Acknowledgements

The research of the second author is partially supported by a grant of the Dynasty Foundation and by the grant "Leading Scientific Schools" NSh-4833.2014.1.

References

[1] M. Baake, U. Grimm: *Aperiodic Order. A Mathematical Invitation*, Cambridge University Press (2013).
[2] L. Bieberbach: Über die Bewegungsgruppen der Euklidischen Räume. (Erste Abhandlung), *Math. Ann.* 70 (1911) 297-336.
[3] L. Bieberbach: Über die Bewegungsgruppen der euklidischen Räume. (Zweite Abhandlung.) Die Gruppen mit einem endlichen Fundamentalbereich, *Math. Ann.* 72, (1912) 400-412.
[4] K. Böröczky: Gömbkitöltések állandó görbületü terekben I, II, *Mat. Lapok* 25 (1974) 265-306, 26 (1974) 67-90.
[5] H. Brugiel, J.H. Conway, C. Goodman-Strauss: *Symmetry of Things*, A.K. Peters, Wellesley MA (2008).
[6] N. Dolbilin, D. Frettlöh: Properties of generalized Böröczky tilings in high dimensional hyperbolic spaces, *European J. Combin.*, 31 (2010) 1181-1195.
[7] N. Dolbilin, D. Schattschneider: The local theorem for tilings, in: *Quasicrystals and discrete geometry*, Fields Inst. Monogr. 10, AMS, Providence, RI (1998) pp 193-199.
[8] D. Schattschneider, N. Dolbilin: One corona is enough for the Euclidean plane, in: *Quasicrystals and discrete geometry*, Fields Inst. Monogr. 10, AMS, Providence, RI (1998) pp 207-246.
[9] N. Pytheas Fogg: *Substitutions in Dynamics, Arithmetics and Combinatorics*, Lecture Notes in Mathematics 1794, Springer, Berlin (2002).
[10] D. Frettlöh, A. Glazyrin: The lonely vertex problem, *Contributions to Algebra and Geometry*, 50 (2009) 71-79.
[11] B. Grünbaum, G.C. Shephard, *Tilings and patterns*, W.H. Freeman, New York (1987).
[12] H. Heesch: Aufbau der Ebene aus kongruenten Bereichen, *Nachr. Ges. Wiss. Göttingen (2)* 1 (1935) 115-117.
[13] K. Reinhardt: *Über die Zerlegung der Ebene in Polygone*, Dissertation Univ. Frankfurt a. M., Borna-Leipzig (1918).
[14] Wikipedia: Orbifold notation, `http://en.wikipedia.org/wiki//Orbifold_notation`, version of 22. Oct. 2013.

Appendix A. Two-dimensional face-to-face monocoronal tiling

In this section we will list all possible monocoronal tilings of the Euclidean plane. The tilings are grouped with respect to (a) the number of polygons incident to the central vertex and (b) the type of this polygons. The caption of any figure will contain (NC) if the depicted tilings may have a non-crystallographic symmetry group, i.e., whether there is a 1-periodic tiling in the class of depicted tilings. The caption will contain (D) if all vertex coronae are directly congruent. Note, that if the vertex corona is mirror symmetric, then all vertex corona are directly congruent.

A.1. Six triangles. We will divide this case further into subcases with respect to the number of different edge lengths occurring. It is easy to see that the case with six different edge lengths incident to each vertex is impossible.

A.1.1. Five edge lengths. There is only one possible case of that type.

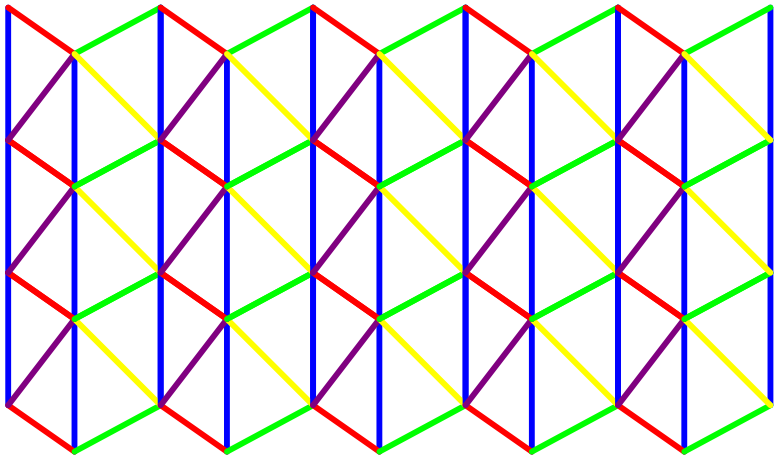

FIGURE 15. Tiling with two different non-isosceles non-reflected triangles (D).

A.1.2. Four edge lengths. First we will list all possible tilings with two pairs of edges of equal length. Here and before we will omit families that can appear as limiting cases of the previous ones. For example here we will not list the case where the yellow edge and the red edge from Figure 15 have the same length.

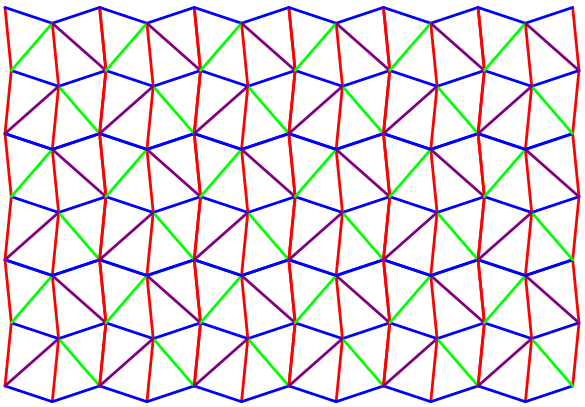

FIGURE 16. Tiling with two different types of non-isosceles triangles.

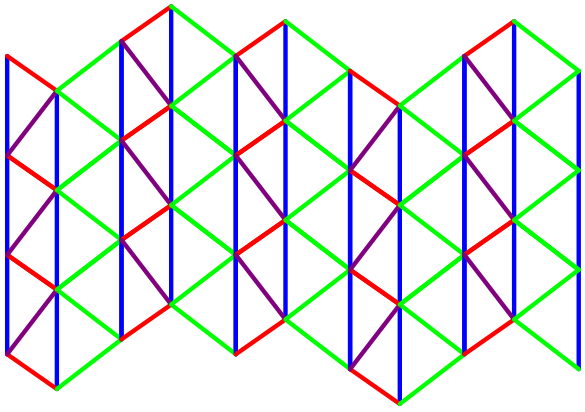

FIGURE 17. Tiling with two types of triangles: one is non-isosceles and one is isosceles (NC).

The only family of this type with three edges of equal length incident to each vertex can be obtained from Figure 15 by forcing the yellow edge and the blue edge to have the same length.

A.1.3. Three edge lengths. This part we start from tilings where each vertex is incident to three pairs of equal edges.

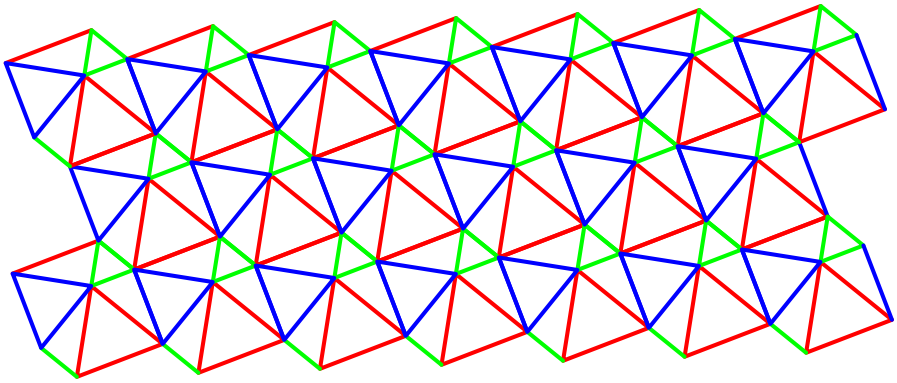

FIGURE 18. Tiling with three different regular triangles and one type of non-isosceles triangle (D).

The second option is the following: each vertex is incident to three edges of the first type, two edges of the second type and one edge of the third type. But this case is covered by families that we listed before.

The third case where each vertex is incident to four equal edges is also covered by previous cases.

A.1.4. Two edge lengths. This is also covered by previous families.

A.1.5. One edge length. This case is trivial since there is only such tiling, namely the canonical tiling by regular triangles.

A.2. Five polygons: three triangles and two quadrilaterals. First we will list all possible tilings where quadrilaterals are consecutive in every vertex-corona.

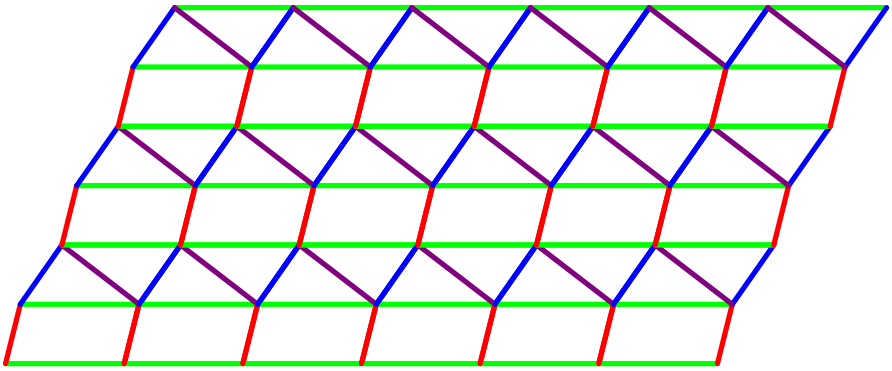

FIGURE 19. Tiling with two equal parallelograms and three equal triangles (D).

Two different limiting cases of this corona can generate non-crystallographic tilings, see Figure 9 for one example. However, if we combine two limiting cases then we will obtain again a crystallographic tiling with rectangles and isosceles triangles.

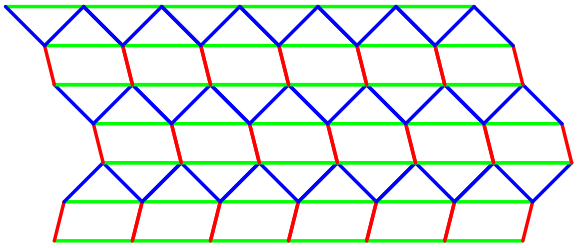

FIGURE 20. Tiling with two equal non-rectangular parallelograms and with three equal isosceles triangles (NC).

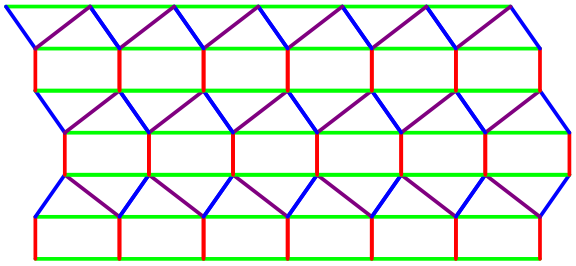

FIGURE 21. Tiling with two equal rectangles and three equal non-isosceles triangles (NC).

The second family consists of tilings whose coronas contain non-consecutive quadrilaterals. There are two different families of such tilings.

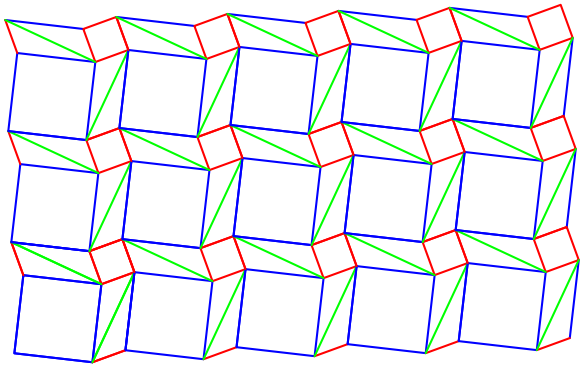

FIGURE 22. Tiling with two different squares and with three equal triangles (D).

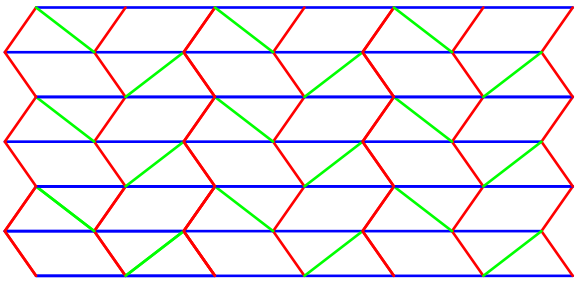

FIGURE 23. Tiling with two equal (non-consecutive) parallelograms and three equal triangles.

A.3. Five polygons: four triangles and one hexagon. There is only one family of such tilings. The vertex corona consists of a regular hexagon, one regular triangle and one arbitrary triangle.

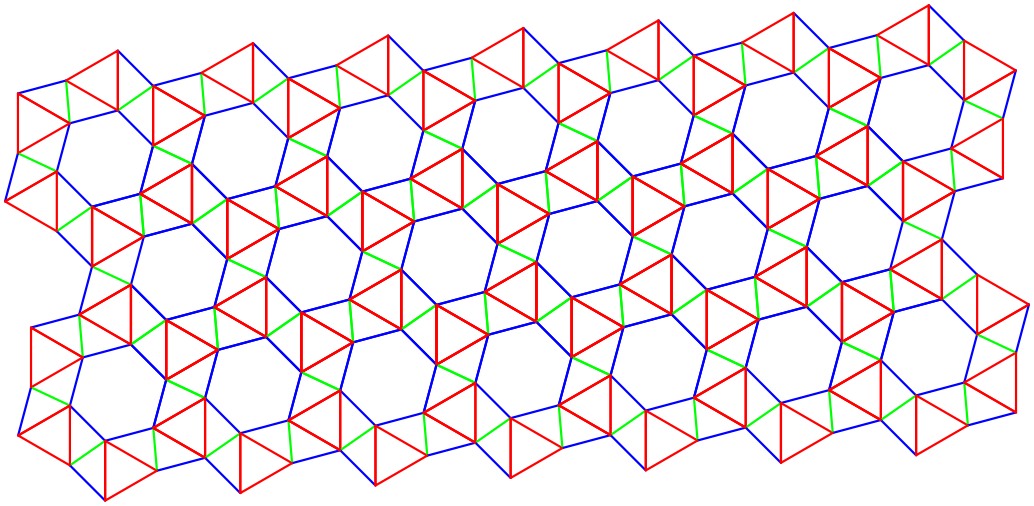

FIGURE 24. Tiling with regular hexagon, regular triangle and an arbitrary triangle (D).

A.4. Four polygons: two triangles and two hexagons. There is only one family of such tilings. Its vertex corona consists of two regular triangles (of different size) and one hexagon with alternating edges and angles.

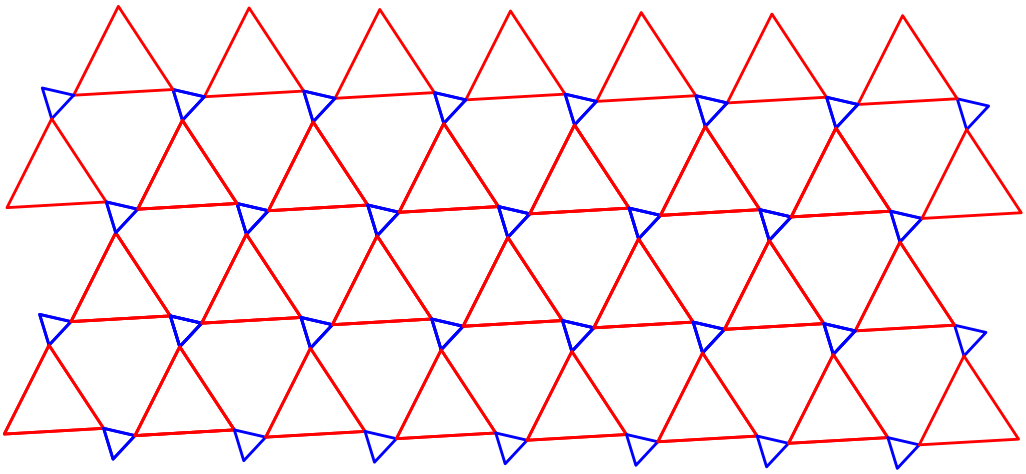

FIGURE 25. Tiling with two types of regular triangles and equal hexagons (D).

A.5. Four polygons: triangle, two quadrilaterals and one hexagon. There are two families of this type. This was shown in Section 2. The first family has a vertex corona consisting of a hexagon with two different edge lengths and the second one consists of hexagons with unique edge length.

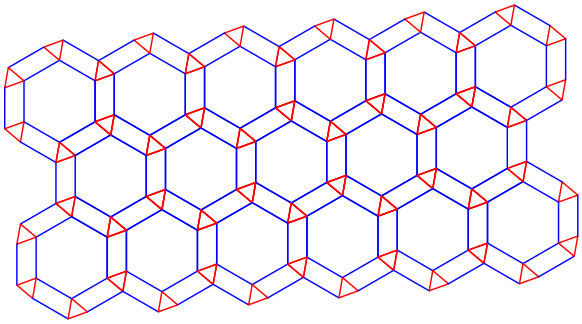

FIGURE 26. Tiling with regular triangle, regular hexagon and two parallelograms (D).

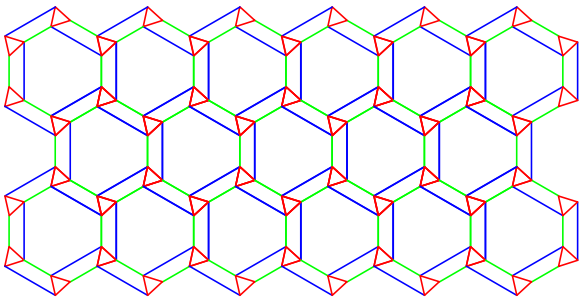

FIGURE 27. Tiling with regular triangle, hexagon and two equal trapezoids.

A.6. Four polygons: four quadrilaterals. In the first part all edges incident to one vertex will be of pairwise different length.

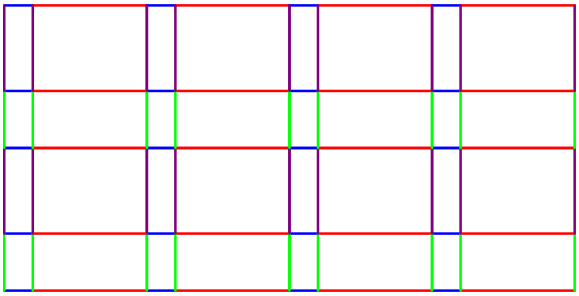

FIGURE 28. All quadrilaterals are rectangles.

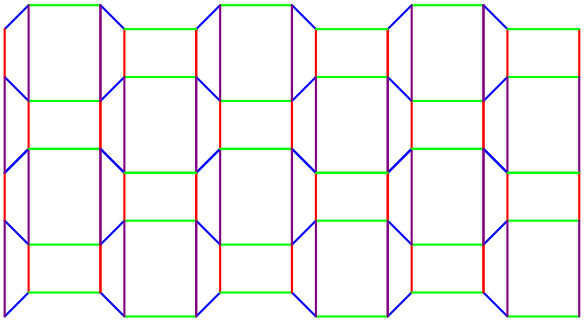

FIGURE 29. The vertex corona consists of two rectangles and two equal trapezoids.

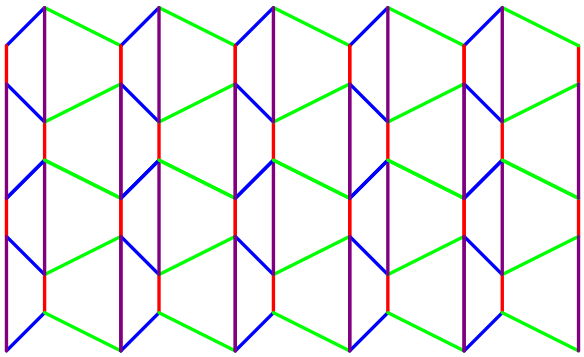

FIGURE 30. Tiling with two types of trapezoids.

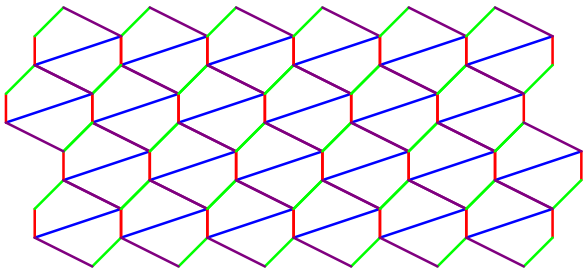

FIGURE 31. Tiling with equal quadrilaterals (D).

Now we list additional families that appear when we allow two edges incident to one vertex to be of equal length (Figures 32, 33, 34, and 35).

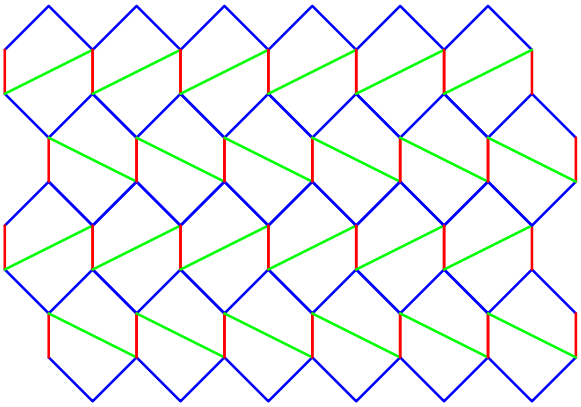

FIGURE 32. Tiling with equal quadrilaterals with reflections.

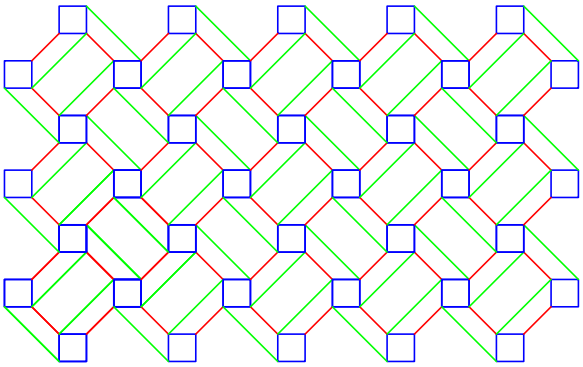

FIGURE 33. Tiling with square, rectangle and two trapezoids.

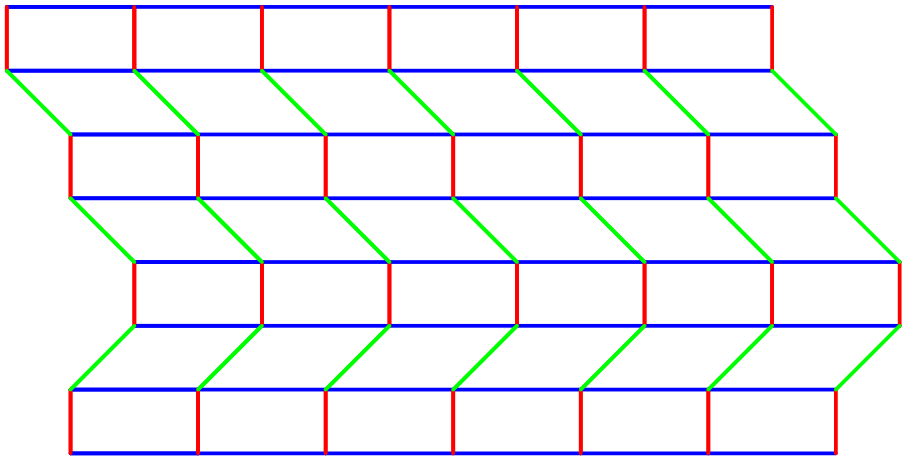

FIGURE 34. A pair of opposite edges in the vertex corona are of the same length and there are two different tiles. Then the tiles are parallelograms. (NC) if one of the parallelograms is a rectangle.

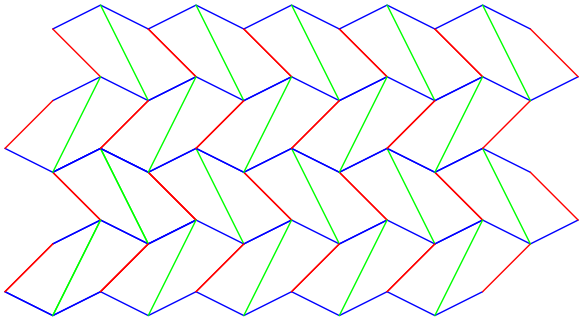

FIGURE 35. A pair of opposite edges are equal and all tiles are equal.

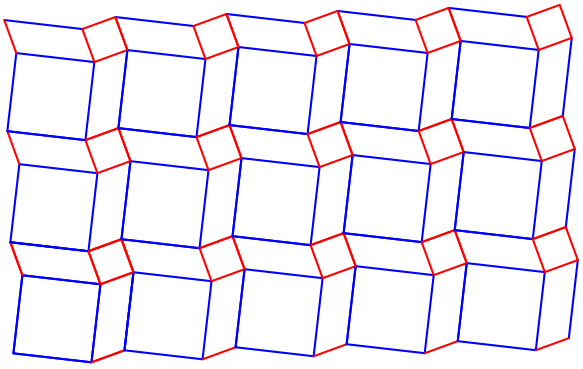

FIGURE 36. Tiling with two different squares and equal parallelograms (D).

The families of tilings with four quadrilaterals at each vertex and with two different edge lengths are covered by previous cases, together with the tiling in Figure 36.

All families of tilings with a single edge length are limit cases of the previous cases.

A.7. Three polygons: triangle and two 12-gons. In this part we will list possible tilings with vertex coronas consisting of one triangle and two 12-gons.

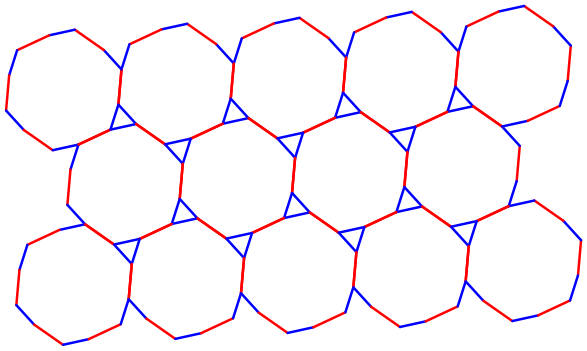

FIGURE 37. Angles of both 12-gons are alternating (D).

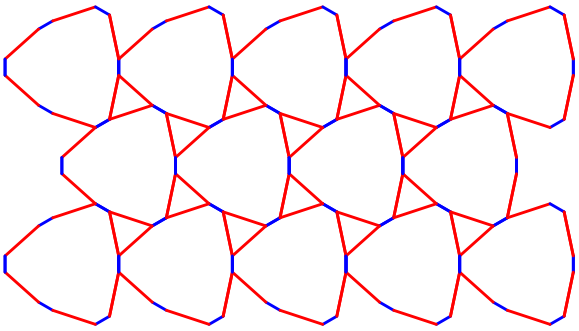

FIGURE 38. Some consecutive angles of 12-gons are equal.

A.8. Three polygons: quadrilateral, hexagon and 12-gon. There is only one family of tilings with vertex corona consisting of quadrilateral, hexagon and 12-gon.

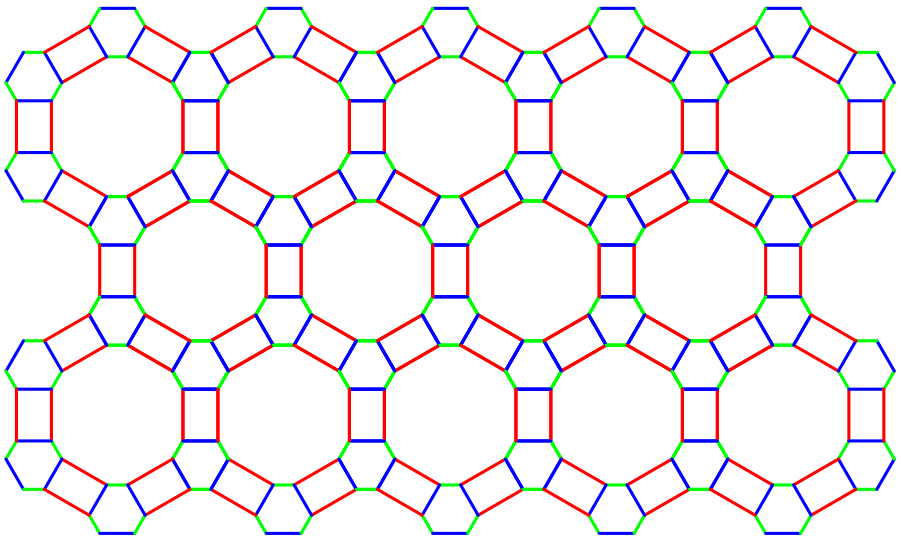

FIGURE 39. Tiling with congruent coronas consisting of quadrilateral, hexagon and 12-gon.

A.9. Three polygons: quadrilateral and two octagons. Every vertex is incident to three edges, two of them are joint edges of a quadrilateral and an octagon. First we list all tilings where these two edges are different.

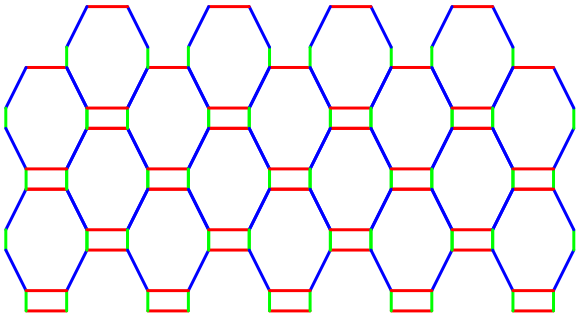

FIGURE 40. Octagons has edges from both families green and red.

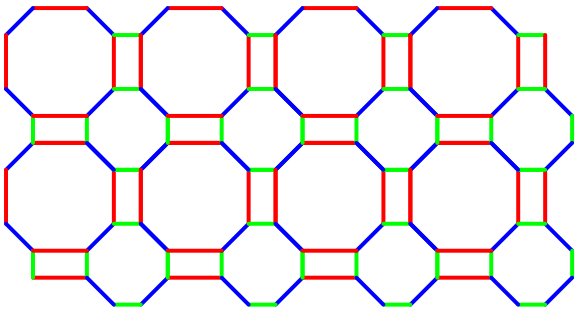

FIGURE 41. Each octagon contains edges only from one family either red or green.

The second case contains families with equal edges between quadrilaterals and octagons.

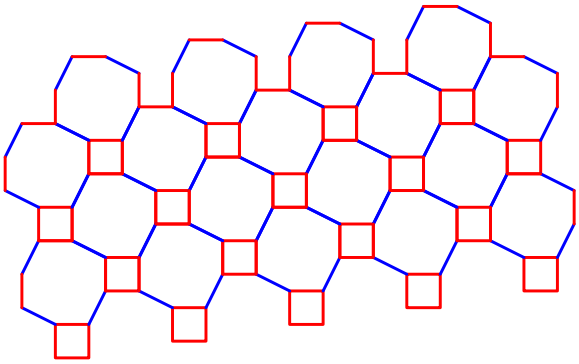

FIGURE 42. Angles of both octagons are alternated.

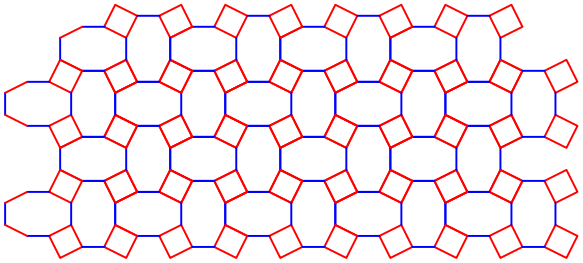

FIGURE 43. Some consecutive angles of octagons are equal.

A.10. Three polygons: three hexagons. In this subsection we present all possible families of tilings with congruent vertex coronas consisting of three hexagons. Each family has a short description of the most important metrical properties.

The first group contains the tilings where all three edges incident to one vertex have different length.

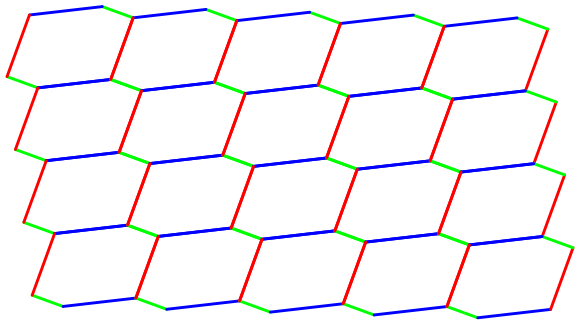

FIGURE 44. All hexagons are translations of each other (D).

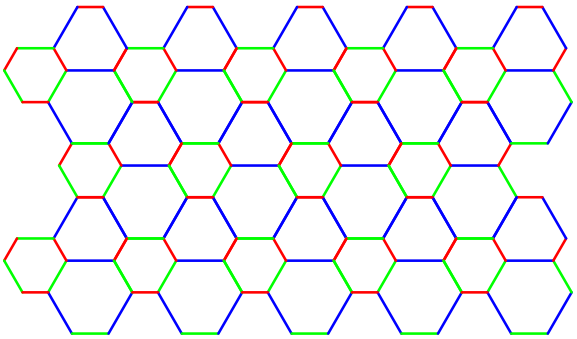

FIGURE 45. All hexagons are different and have alternating colourings.

In the sequel we list the possible families with two equal edges incident to every vertex. We omit those tilings that can be achieved from previously described families (Figures 44–46) by letting two different edges to be of equal lengths without using the additional degree of freedom obtained from the possibility of having different angles.

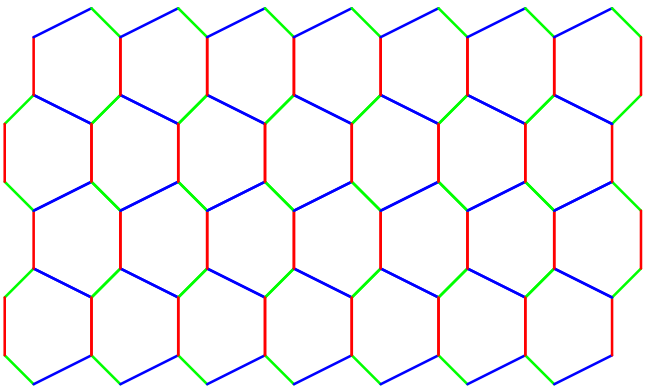

FIGURE 46. Hexagons are the same but odd rows are reflected.

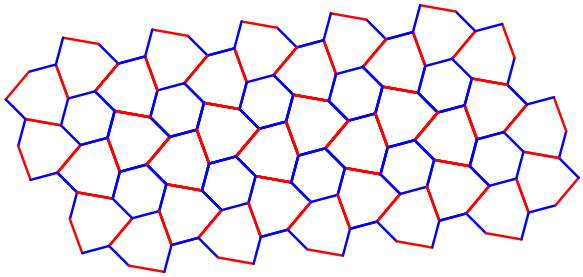

FIGURE 47. Two incident edges are equal (D).

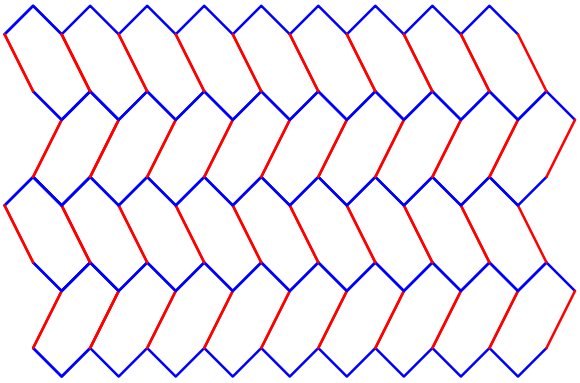

FIGURE 48. Two edges are of equal length. This allows using reflected coronae with respect to the case in Figure 44.

The cases where all edges are of equal length are obtained from the previous cases by letting some different edge lengths to be equal. For example, if we force all edges in Figure 45 to be equal then we will obtain the tiling by regular hexagons.

Appendix B. Non face-to-face monocoronal tiling

Here we list all possible families of non face-to-face monohedral tilings. We will group them with respect to polygons that are incident to each vertex (except the one polygon that contributes not a vertex, but an edge).

B.1. Triangle and hexagon. We start from the case where each hexagon is regular.

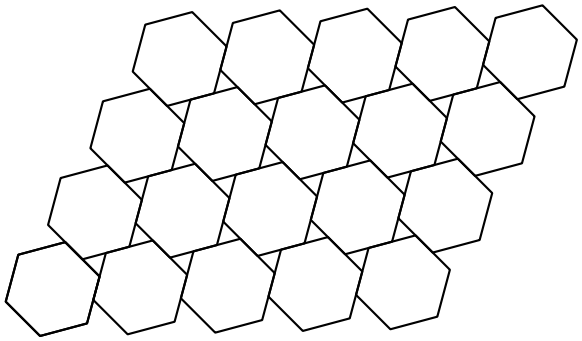

FIGURE 49. Tiling with regular hexagon and regular triangle. The edge of the hexagon is longer (D).

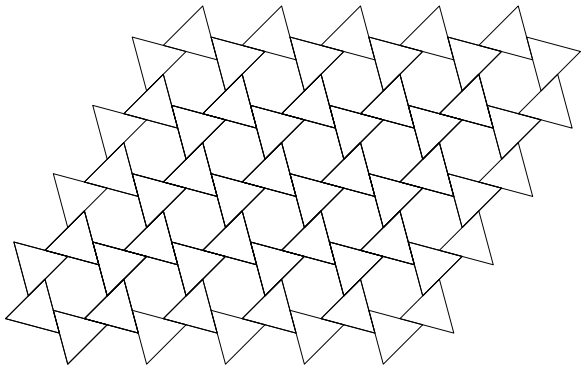

FIGURE 50. Tiling with regular hexagon and regular triangle. The edge of the hexagon is shorter (D).

The second case is when the hexagon is non-regular. In that case any of its longer side touches two equal regular triangles.

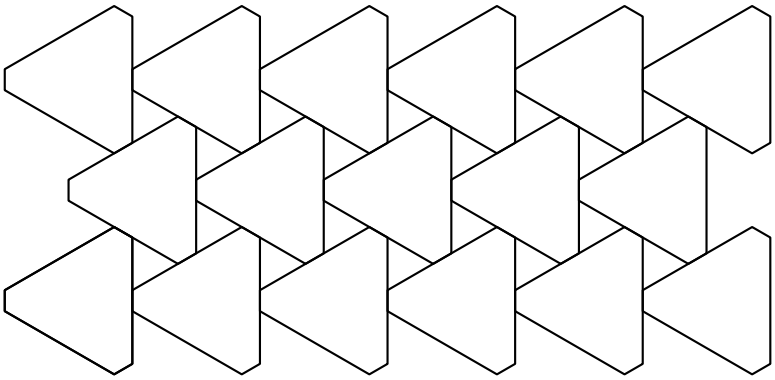

FIGURE 51. Tiling with regular triangle and non-regular hexagon.

B.2. Two quadrilaterals. There are two significantly different cases: the intersection of two quadrilaterals incident to the vertex is an entire edge of both of them, or it is an entire edge of one of them and only a part of an edge of the other. We start our list with the first case.

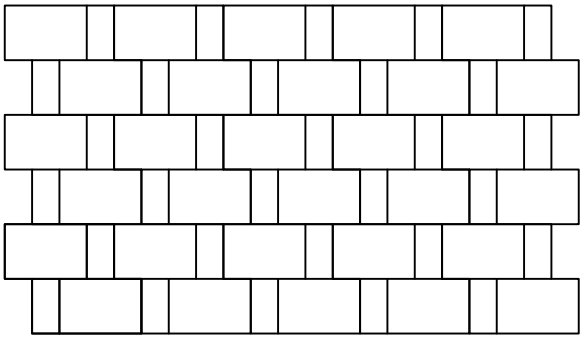

FIGURE 52. Tiling with two types of rectangles.

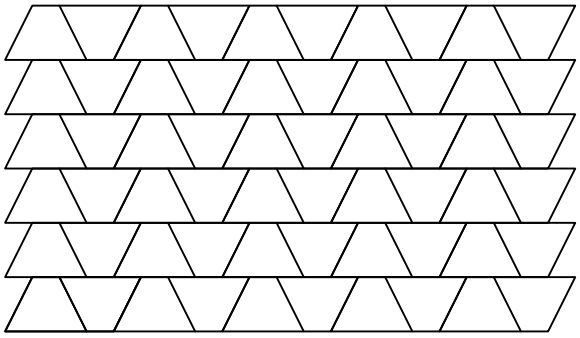

FIGURE 53. Tiling with one type of trapezoid.

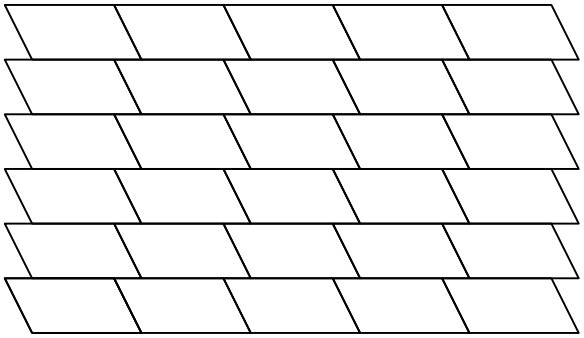

FIGURE 54. Tiling with one type of parallelogram (D).

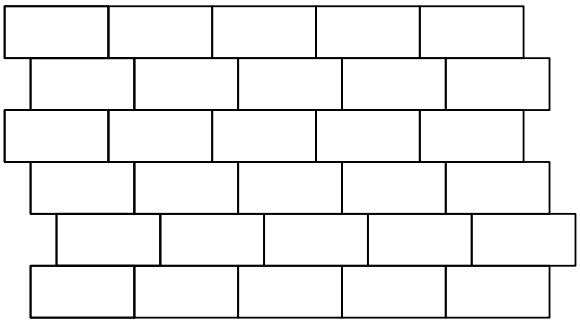

FIGURE 55. Tiling with one type of rectangle (NC).

And there are two additional tilings for the second case.

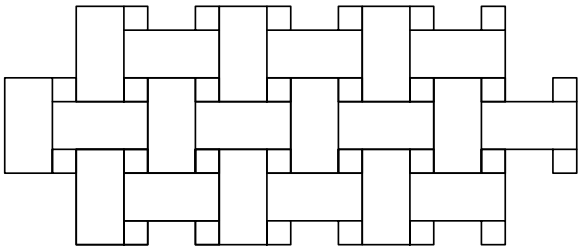

FIGURE 56. Tiling with square and rectangle.

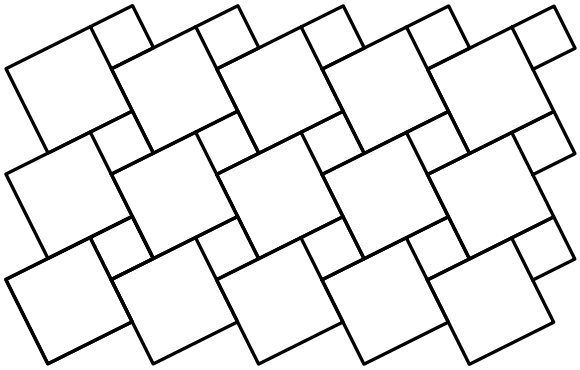

FIGURE 57. Tiling with two types of squares (D).

B.3. Three triangles. As in the previous case the tilings are combined into families with similar incidence structure of the vertex corona.

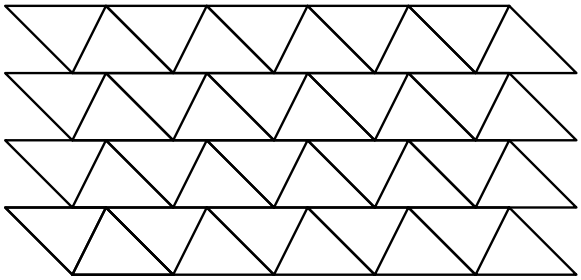

FIGURE 58. Tiling with one type of arbitrary triangle (D).

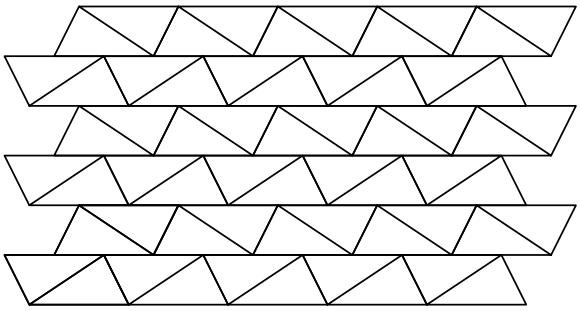

FIGURE 59. Tiling with one type of arbitrary triangle but odd rows are reflected.

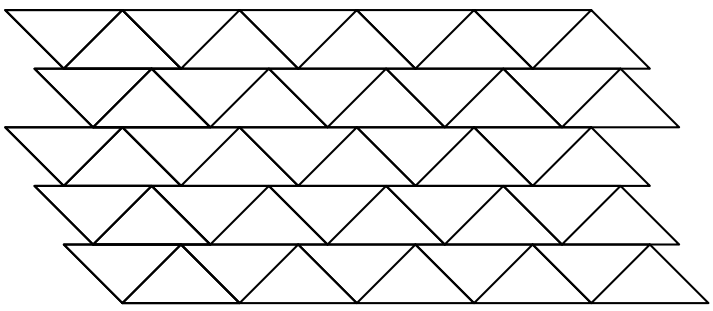

FIGURE 60. Tiling with isosceles triangles (NC).

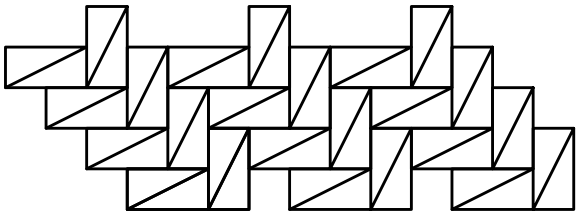

FIGURE 61. Tiling with one type of arbitrary triangle. Two triangles in the vertex corona share an entire long edge, the other two share part of a medium edge.

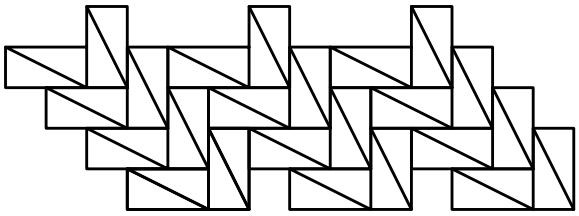

FIGURE 62. Tiling with one type of arbitrary triangle. Two triangles in the vertex corona share an entire long edge, in the other two a medium edge touches a short edge.

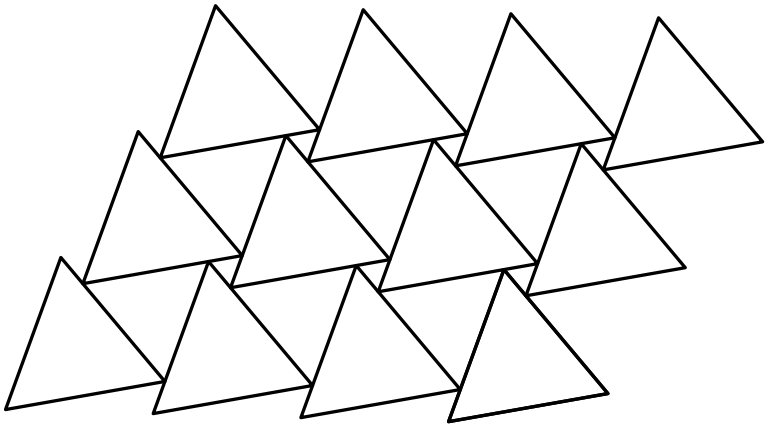

FIGURE 63. Tiling with three types of regular triangles (D).

Appendix C. Tilings with symmetry groups $*\!*$, $\times\times$, and $\circ$

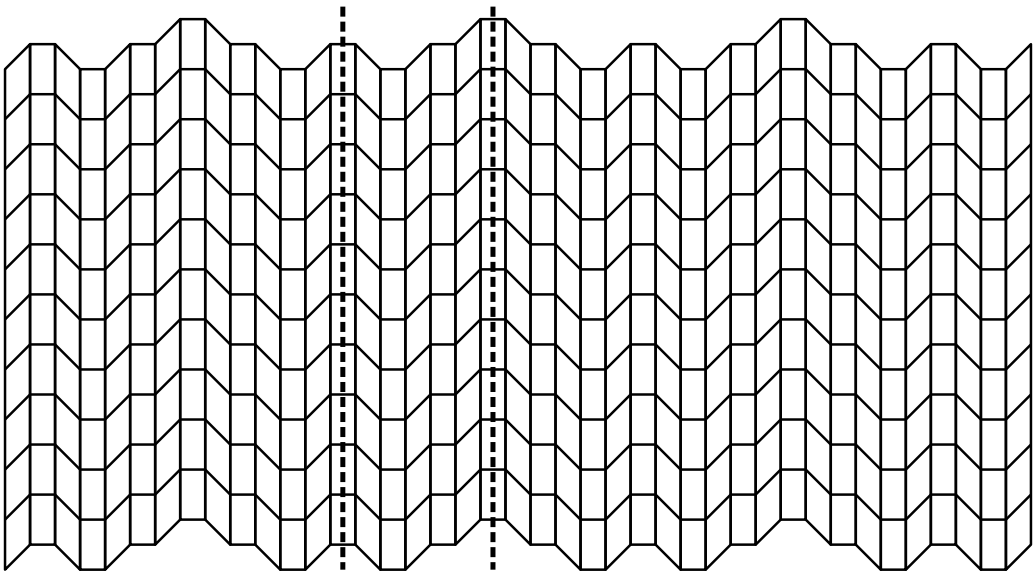

FIGURE 64. A crystallographic tiling where layers repeat according to the periodic sequence $\ldots 101100 \ldots$. It is invariant under mirror reflection in the two axes indicated by dashed lines.

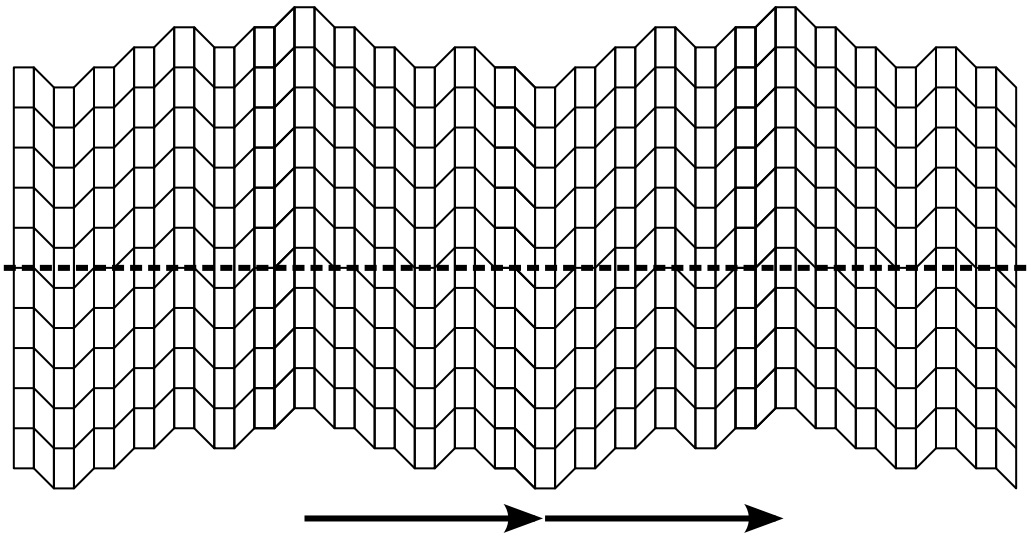

FIGURE 65. A crystallographic tiling where layers repeat according to the periodic sequence ...111011000100.... It is not invariant under any reflection, but it is invariant under a glide reflection: a reflection in the axis indicated by the dashed line, followed by a translation indicated by one of the arrows.

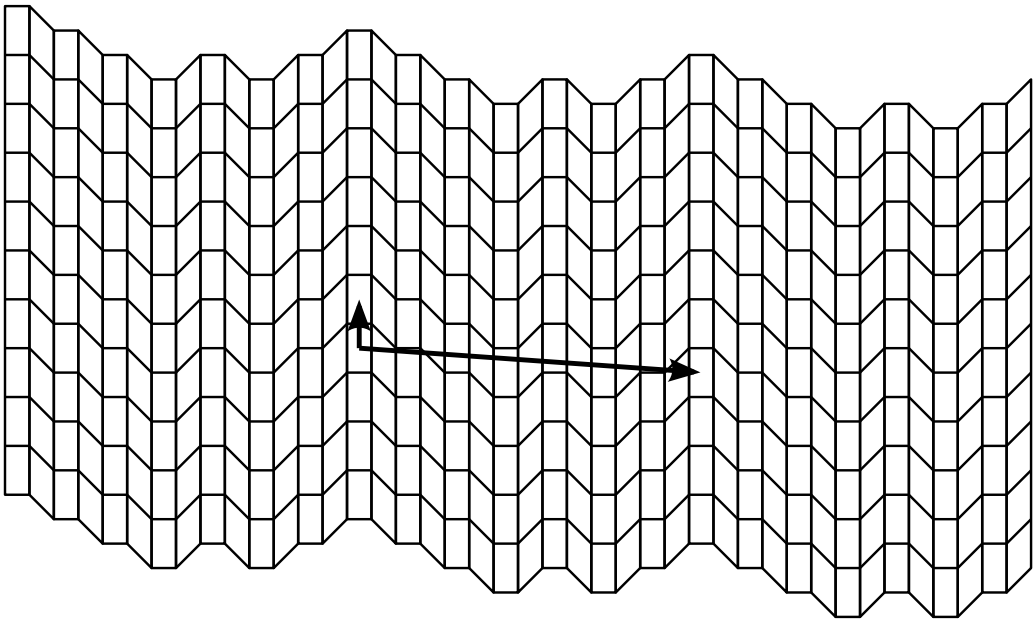

FIGURE 66. A crystallographic tiling where layers repeat according to the periodic sequence ...0001011.... Its symmetry group contains translations only. The arrows in the image indicate two translation that generate the entire symmetry group.

TECHNISCHE FAKULTÄT, UNIV. BIELEFELD

E-mail address: dirk.frettloeh@udo.edu

DEPARTMENT OF GEOMETRY AND TOPOLOGY, FACULTY OF MECHANICS AND MATHEMATICS, MOSCOW STATE UNIVERSITY

E-mail address: alexeygarber@gmail.com